Original Article

Effects of acupuncture on the miR-146a-mediated IRAK1/TRAF6/NF-κB signaling pathway in rats with sarcopenia induced by D-galactose

Jing Jin[1#], Zhengyu Yang[1#], Haichao Liu[1], Mingling Guo[2], Borui Chen[1], Haoming Zhu[1], Yu Wang[1], Jianping Lin[2], Shizhong Wang[2], Shaoqing Chen[1]

[1]College of Rehabilitation Medicine, Fujian University of Traditional Chinese Medicine, Fuzhou, China; [2]The School of Health, Fujian Medical University, Fuzhou, China

Contributions: (I) Conception and design: S Chen, J Lin, S Wang; (II) Administrative support: S Wang; (III) Provision of study materials or patients: S Chen; (IV) Collection and assembly of data: J Jin, M Guo, Z Yang, B Chen, H Zhu, Y Wang, H Liu; (V) Data analysis and interpretation: J Jin, Z Yang; (VI) Manuscript writing: All authors; (VII) Final approval of manuscript: All authors.

[#]These authors contributed equally to this work and should be considered as co-first authors.

Correspondence to: Jianping Lin; Shizhong Wang. The School of Health, Fujian Medical University, Fuzhou, China. Email: ljp1985@fjmu.edu.cn; shzhwang@fjmu.edu.cn; Shaoqing Chen. College of Rehabilitation Medicine, Fujian University of Traditional Chinese Medicine, Fuzhou, China. Email: chensq@fjtcm.edu.cn

Background: Sarcopenia during aging is closely linked to sterile, low-grade, chronic inflammation. However, considering the increasingly aging global population, the effectiveness of existing treatments for sarcopenia is not exact, and acupuncture, as an effective anti-inflammatory therapy, has the potential to treat it.

Methods: Fifty Sprague-Dawley rats were randomly allocated into five groups, including Control group, D-galactose (D-gal) group, D-gal + acupuncture (DA) group, D-gal + non-acupoint (DN) group and D-gal amino acid mixture (DAA) group. An aging rat was model constructed using D-gal for 12 weeks. Rats in the control group received 0.9% physiological saline daily. Treatment groups were acupunctured or given amino acid mixture interventions daily, and lasted for last 4 consecutive weeks. The effects of acupuncture were evaluated by the hematoxylin and eosin staining (H&E), transmission electron microscopic (TEM) examination and terminal deoxynucleotidyl transferase dUTP nick end labeling (TUNEL) assays. The anti-inflammatory mechanism of acupuncture was studied by using the expressions of microRNA-146a (miR-146a) mediated nuclear factor-kappa B (NF-κB) signaling pathway-related proteins were detected by immunofluorescence, western blotting, quantitative real-time polymerase chain reaction (PCR) and enzyme-linked immunosorbent assay (ELISA).

Results: Rats injected by D-galactose (D-gal) revealed apparent skeletal muscle atrophy with significantly reduced cross-sectional area and fiber diameter. In contrast, acupuncture treatment alleviated these hallmarks of skeletal muscle atrophy and mitigated the mitochondrial aberrations and skeletal muscle apoptosis in D-gal rats. In addition, acupuncture also downgraded the overexpression of inflammatory factors in skeletal muscle, influenced miR-146a and the target genes level, and inhibited NF-κB nuclear translation in D-gal rats.

Conclusions: Acupuncture may ameliorate skeletal muscle atrophy, and its effects may be associated with the control of mitochondrial function regulation and the suppression of inflammation.

Keywords: Aging; sarcopenia; acupuncture; microRNA-146a; nuclear factor-kappa B (NF-κB)

Submitted Nov 16, 2022. Accepted for publication Jan 03, 2023. Published online Jan 13, 2023.
doi: 10.21037/atm-22-6082
View this article at: https://dx.doi.org/10.21037/atm-22-6082

Introduction

Skeletal muscle is an essential tissue responsible for physical function and metabolic health. Age-related muscle atrophy leads to the reduction of muscle mass and function, a phenomenon termed sarcopenia, which impacts the life quality of the elderly by decreasing movement and increasing muscle weakness (1,2). Furthermore, sarcopenia is closely associated with many comorbidities, such as Parkinson's disease, peptic ulcer disease, diabetes mellitus, and chronic obstructive pulmonary disease (3-6), which may clarify why it is linked to a variety of age-related outcomes, including cognitive impairment and a higher chance of hospitalization and all-cause mortality (7). Recent research has discovered a clear correlation between greater levels of circulating inflammatory markers and lower, decreasing levels of skeletal muscle mass (8).

Advancing age has been reported to be linked to a condition of chronic low-grade inflammation in various tissues (9), which is known as "inflammaging" and characterized by elevated levels of circulating pro-inflammatory mediators (10), including the cytokines interleukin 1β (IL-1β), tumor necrosis factor-α (TNF-α), and IL-6 (11,12). As an important transcription factor for apoptosis, immunity, and inflammation (13), nuclear factor-kappa B (NF-κB), as a decisive molecule in muscle atrophy (14), has been illustrated to be activated in multiple organs of the elderly and aging animals, including aged muscles (15,16). Age-related increases in NF-κB activity appear to be a common biological phenomenon, and NF-κB might be a pathogenic component for a variety of illnesses (17-19). Notably, NF-κB activation has been observed in D-galactose (D-gal)-induced aging models (20,21). MicroRNA-146a (miR-146a) was the first NF-κB-dependent microRNA (miRNA) to be discovered (22), and has been found to downregulate the expression of typical NF-κB pathway proteins, such as the toll like receptor 4 (TLR4), TNF receptor-associated factor 6 (TRAF6), and the IL-1 receptor-associated kinase 1 (IRAK1) (23,24). On the other hand, miR-146a also targets RelB, which plays a crucial role in the non-canonical NF-κB pathway (25,26). Accordingly, the capacity of miR-146a to influence the NF-κB pathways qualifies it as a candidate for biomarker inflammation. Moreover, targeted miR-146a deletion in mice can result in NF-κB-driven inflammation that arises naturally with aging, and upregulation of systemic inflammatory factors further leads to skeletal muscle atrophy (27,28). Over all, inflammation-related miR-146a level is directly related to muscle strength in the ageing creatures, and it is serving as critical bio-markers of age-related sarcopenia.

Mitochondria are key organelles regulating skeletal muscle metabolism and can damage or kill their hosts by producing reactive oxygen species (ROS) or pro-inflammatory signals (29), and mounting evidence suggests they are essential for inflammatory phenotype development (30). Pyrin domain containing 3 (NLRP3) inflammasomes belong to the NOD-like receptor family, and evidence of their activation has been reported in a wide range of age-related conditions (31). Furthermore, a study suggested the ROS produced from mitochondria have a role in NLRP3 activation (32). In addition, mitochondrial ROS production has been demonstrated to impede protein synthesis via reducing phosphorylation of the 4e-binding protein and affecting the mammalian target of rapamycin (mTOR) assembly (33), causing significant disruptions in muscle remodeling and mitochondrial fission and inducing muscular atrophy (34).

Acupuncture, a traditional Chinese therapy with a history of over 3,000 years, has been increasingly used as an integrative or complementary therapy worldwide (35). As a low-cost, well-tolerated therapy with few and minor adverse effects, acupuncture has a certain regulatory influence on systemic inflammation (36-38). The anti-inflammatory impact of acupuncture is mediated through the activation of the immune response at acupoints (39), and evidence indicates expressions of NF-κB are downregulated and miR-146a is upregulated after acupuncture treatment

Highlight box

Key findings

- Acupuncture improves D-gal-induced skeletal muscle atrophy and influences the inflammation induced by microRNA-146a (miR-146a)-mediated nuclear factor-kappa B (NF-κB).

What is known and what is new?

- Previous studies have found D-gal injection can cause skeletal muscle atrophy and mitochondrial aberration in rats.
- This study finds that acupuncture inhibited D-gal-induced skeletal muscle atrophy, delayed the age-induced mitochondrial dysfunction of skeletal muscle, and alleviated apoptosis of the muscle nucleus. Acupuncture also upregulate miR-146a and downregulate of the expression of the IRAK1/TRAF6/NF-κB pathway and related inflammatory factors.

What is the implication, and what should change now?

- Targeting the miR-146a-mediated IRAK1/TRAF6/NF-κB pathway by acupuncture treatment may have inhibited D-gal-induced skeletal muscle atrophy, which may provide an optimistic therapeutic strategy for less intrusive and more effective therapy for musculoskeletal disorders.

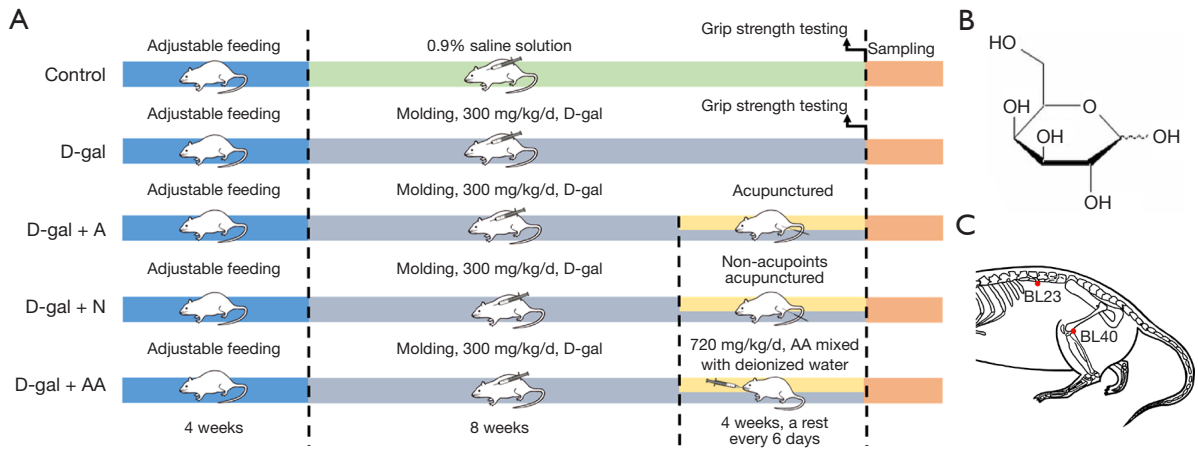

Figure 1 Flow chart and details of the experiment. Flow chart of this experiment (A). Molecular formula of D-galactose (B). Location map of BL23 and BL40 (C). D-gal, D-galactose; A, acupuncture; N, non-acupoint; AA, amino acid.

(40,41). Nevertheless, it remains unclear how acupuncture prevents sarcopenia and inflammaging. Here, we propose the hypothesis that acupuncture improves skeletal muscle atrophy and modulates the miR-146a-mediated TRAF6/NF-κB signaling pathway to inhibit inflammatory responses. We present the following article in accordance with the ARRIVE reporting checklist (available at https://atm.amegroups.com/article/view/10.21037/atm-22-6082/rc).

Methods

Experimental animals and environment

Fifty mature male Sprague-Dawley 8 weeks rats (body weight: 200±20 g) were acquired from the Shanghai SLAC Co., Ltd. (Shanghai, China). All experiments were performed under a project license (No. FJTCM IACUC 2021053) granted by Ethics Committee of Fujian University of Traditional Chinese Medicine, in compliance with institutional guidelines for the care and use of animals. A protocol was prepared before the study without registration.

Standard laboratory settings were employed for rat housing, which included a constant humidity between 40% and 60%, a temperature of 22 ℃, and a light-dark cycle of 12 hours. Each cage contained five rats, and food pellets and water were freely available. As listed in (*Figure 1A*), after adapting to the new environment for 4 weeks, rats aged approximately 12 weeks and weighing 330±20 g were uniquely numbered, and then randomly allotted into five groups (n=10 each group) grouped with SPSS without any other information or tendencies involved: control group (300 mg/kg/d 0.9% normal saline, subcutaneous injection); D-galactose group (D-gal group; 300 mg/kg/d D-gal, subcutaneous injection); D-gal acupuncture group (DA); D-gal non-acupoint control group (DN); and D-gal amino acid mixture group (DAA) (720 mg/kg/d, intragastric administration). In detail, rats in the D-gal, DA, DN, and DAA groups were injected subcutaneously in the nape of neck with 300 mg/kg of D-gal dissolved in saline solution (>99% purity; No. S11050; Yuanye Bio-Technology Co. Ltd., Shanghai, China) daily for 12 weeks, with the dosage of D-gal based on a previous study (42). Rats in the control group received 0.9% physiological saline solution (300 mg/kg/d, i.h) daily for 12 weeks.

Interventions

In the DA, DN, and DAA groups, interventions commenced on the ninth week of the 12-week D-gal subcutaneous injection protocol. The molecular formula of D-gal is shown in *Figure 1B*. The fur of each rat in the DA and DN groups was shaved at the appropriate area using an electrical shaver before the first treatment to reveal acupoints or non-acupoints. Rats were wrapped in fitted and soft fabric materials and fastened in the prone position in a conscious condition using a self-made rat fixator during DA and DN therapy. Single-use sterile acupuncture needles 25 mm long and 0.25 mm in diameter were used. Rats in the DA group were administered acupuncture at the bilateral Weizhong (BL40; stab to a depth of 7–8 mm at the popliteal crease midway, and biceps femoris tendon and the semitendinosus tendon midpoint) and Shenshu (BL23; stab to a depth

Table 1 Table of composition of mixed amino acids

Amino acids	Rat dose, mg/0.2 g	Rat dose, mg/kg
Leucine (LEU)	45	225
Lysine-HCl	23.4	117
Isoleucine (ILE)	22.5	112.5
Valine (VAL)	22.5	112.5
Threonine	12.6	63
Cysteine (CYS)	5.4	27
Histidine (HIS)	5.4	27
Phenylalanine (PHE)	3.6	18
Methionine (MET)	1.8	9
Tyrosine (TYR)	1.08	5.4
Tryptophan (TRP)	0.72	3.6
Total content	144	720

of 4–5 mm at the point 7 mm lateral to the depression below the spinous processes of the two lumbar vertebra) (*Figure 1C*), while those in the DN group were administered the same treatment at another non-acupoint (localized 5 mm below the BL40 acupoint). The acupuncture point locations on rats were identified according to comparative anatomy and experimental acupuncture science (43). Rats in the DA and DN groups received acupuncture for 30 min once daily with rotating manipulation administered every 5 minutes for 10 seconds. At a rate of 90°/s, each needle was spun 90° bidirectionally. As a positive control, rats in the DAA group received a single gavage administration of amino acid mixture (720 mg/kg/d, mixed with deionized water) (*Table 1*). Intervening therapy was given once daily for 4 weeks with a break every 6 days.

Samples and preservation

This experiment was conducted over 16 weeks, at which point 1% pentobarbital sodium (50 mg/kg) was intraperitoneal injected to anesthetize the rats. After dissecting the erector spinae, the blood was rinsed with saline, and a portion of the skeletal muscle was preserved in 4% paraformaldehyde for histological assessment. Another segment of the skeletal muscle was immediately cut into strips with a cross-sectional area of 1–2 mm^3 according to the direction of muscle fibers, then fixed in 2.5% glutaraldehyde for 2 hours at room temperature followed by storage at 4 ℃ without light. For further bioassays, liquid nitrogen was used to snap-freeze the remaining muscle tissue at –80 ℃ in a public refrigerator.

Grip strength test

The grip power of rats' limbs was evaluated using a grip strength meter (XR-YLS-13A; XinRuan Co. Ltd., Shanghai, China). Rats were encouraged to grasp onto a metal grid (23 cm × 25 cm) then steadily dragged backward by the tail at a constant speed until they were unable to grip. Five trials were required of each rat, and the average result was noted as the rat's grip strength. The experiment was performed at the end (week 12) of the trial.

Hematoxylin and eosin (H&E) staining

The morphology of skeletal muscle fibers was explored utilizing H&E. Skeletal muscle was immediately harvested under anesthesia and rinsed in 0.9% saline after trimming adipose tissue and tendons. Subsequently, skeletal muscle was preserved in 4% paraformaldehyde for 24–48 hours (4 ℃), wrapped in paraffin after dehydration with gradient alcohol, then cut into 5-μm paraffinized sections. Slides were dewaxed by a gradient of xylene and alcohol and stained with an H&E kit (Solarbio Science Technology Co., Ltd., Beijing, China) to view the general muscle structure. All DNA/RNA structures bonded to and were stained blue by hematoxylin, while tissue proteins were counterstained pink by eosin. Once stained, the slides were covered with a coverslip before viewing. The average cross-sectional area and the gastrocnemius muscle fibers diameter were analyzed by Image Pro-Plus.

Transmission electron microscopic examination

A 1 mm^3 sample of skeletal muscle was taken, fixed for 2 hours in glutaraldehyde in phosphate buffer (2.5%), washed with a 1 mmol/L phosphoric acid solution, then fixed for 4 hours in osmium tetroxide (1%). The stones were precisely sliced into 0.07 mm thick portions, then 3% uranylacetate and lead citrate were applied to stain the slices, which were then examined using a transmission electron microscope (JEOL JEM1400).

Terminal deoxynucleotidyl transferase nick-end labeling

Paraffinized muscle (thickness, 5 μm) sections were dewaxed

by a gradient of xylene and alcohol, then phosphate buffered saline (PBS) was used to fix the muscle tissue for 20 minutes. We used a Tunel Kit (cat. No. G1504, Servicebio Biological Technology Co. Ltd., Wuhan, China) to stain the terminal deoxynucleotidyl transferase (dUTP) nick-end labeling (TUNEL), and TUNEL-positive cells were counted and expressed as a proportion of all nuclei in each section. Images were captured using 4',6-diamidino-2-phenylindole (DAPI) and fluorescein filter blocks under a ×400 objective Olympus fluorescent microscope (Olympus, Tokyo, Japan). At least 300 chosen cells from each group in each experiment were identified for quantification.

Immunofluorescence assay

Muscle slices (thickness, 5 μm) were infiltrated with anti-NF-κB antibody (1:200 cat. No. ab16502, Abcam). Immunoglobulins with identical concentrations and specific to different species served as the controls (Beyotime Biotechnology Co. Ltd., Shanghai, China). Slices were examined using a fluorescent microscope (Olympus) after being marked with the secondary antibody that was Cy3-tagged.

Western blot

Skeletal muscle was homogenized in Radio Immunoprecipitation Assay (RIPA) lysis buffer containing phosphatase and protease inhibitors. Protein quantification was performed by bicinchoninic acid procedure protein assay (BCA), and sodium dodecyl-sulfate (SDS) polyacrylamide gel electrophoresis was used to isolate equal contents of protein (35 μg for each lane). After activation of the polyvinylidene fluoride (PVDF) membranes, the protein was transferred to the membranes under the condition that the membrane remained moist. A 5% skim milk solution was then used to block the membranes containing the target proteins for 2 h, before incubation with primary antibodies at 4 ℃ overnight, then secondary antibody (1:8,000) for 90 minutes. The membranes were imaged using the Bio-Image Analysis system using an improved chemiluminescence kit (Meilunbio, MA0186, Dalian, China). Reagents from Abcam were as follows: IRAK1 (1:1,000, cat. No. ab238), TRAF6 (1:1,000, cat. No. ab33915), phospho-NF-κB p65 (1:1,000, cat. No. ab76302), NF-κB p65 (1:2,000, cat. No. ab16502), Akt (1:1,000, cat. No. ab8805) and phospho-Akt (1:1,000, cat. No. ab38449), glyceraldehyde-3-phosphate dehydrogenase (GAPDH) (1:6,000, cat. No. 60004-1-Ig, Proteintech Group Inc., Chicago, USA)

Quantitative real-time polymerase chain reaction

Total RNA of rat skeletal muscle (60–80 mg) was obtained using an extraction kit (cat. no. R401-01), and cDNA was created by the HiScript II 1st Strand cDNA Synthesis Kit (cat. No. R211-02). In a thermal cycler (ABI 7500, Thermo Fisher Scientific, Inc., Shanghai, China), quantitative real-time polymerase chain reaction (qPCR) was conducted using a ChamQ Universal SYBR qPCR Master Mix (cat. No. Q711-02,). The reagents used above were obtained from the China Vazyme Biotech Co., Ltd. (Nanjing, China) Each sample's level of U6 expression was evaluated to normalize gene expression for variations in RNA input, RNA quality, and reverse transcription efficiency, and the $2^{-\Delta\Delta Ct}$ relative quantification technique was used to quantify the fold differences in miRNA expression levels across samples. The primer sequences (SunYa Biotechnology Co., Ltd., Zhejiang, China) were as follows (forward and reverse, 5'-3'): U6, CTCGCTTCGGCAGCACATATACT (forward) and ACGCTTCACGAATTTGCGTGTC (reverse); miR-146a-5p, CCGCGCTGAGAACTGAATTCCA (forward) and AGTGCAGGGTCCGAGGTATT (reverse) and GT CGTATCCAGTGCAGGGTCCGAGGTATTCGCACT GGATACGACAACCCA (RT).

Enzyme-linked immunosorbent assay (ELISA) of inflammatory factors in skeletal muscle

The skeletal muscle tissues of rats in each group were homogenized by adding 0.3 mL of 9% normal saline every 10 g. The tissue supernatant was produced by centrifugation, and the concentration of the homogenate derived from the muscle was brought into equilibrium. We used an ELISA kit to detect the levels of IL-6, IL-1β, IL-10, and TNF-α. The measurements were conducted according to the instructions provided by the manufacturer (BOSTER Biological Technology Co. Ltd., Wuhan, China).

Statistical analysis

Data are expressed by the mean ± standard deviation (SD) or the standard error of the mean (SEM). Analysis of variance (ANOVA) analysis was used for group comparisons, and the least significant difference test (LSD-t) and Games-Howell test were used to conduct the analysis of pairwise comparisons according to the results of homogeneity of

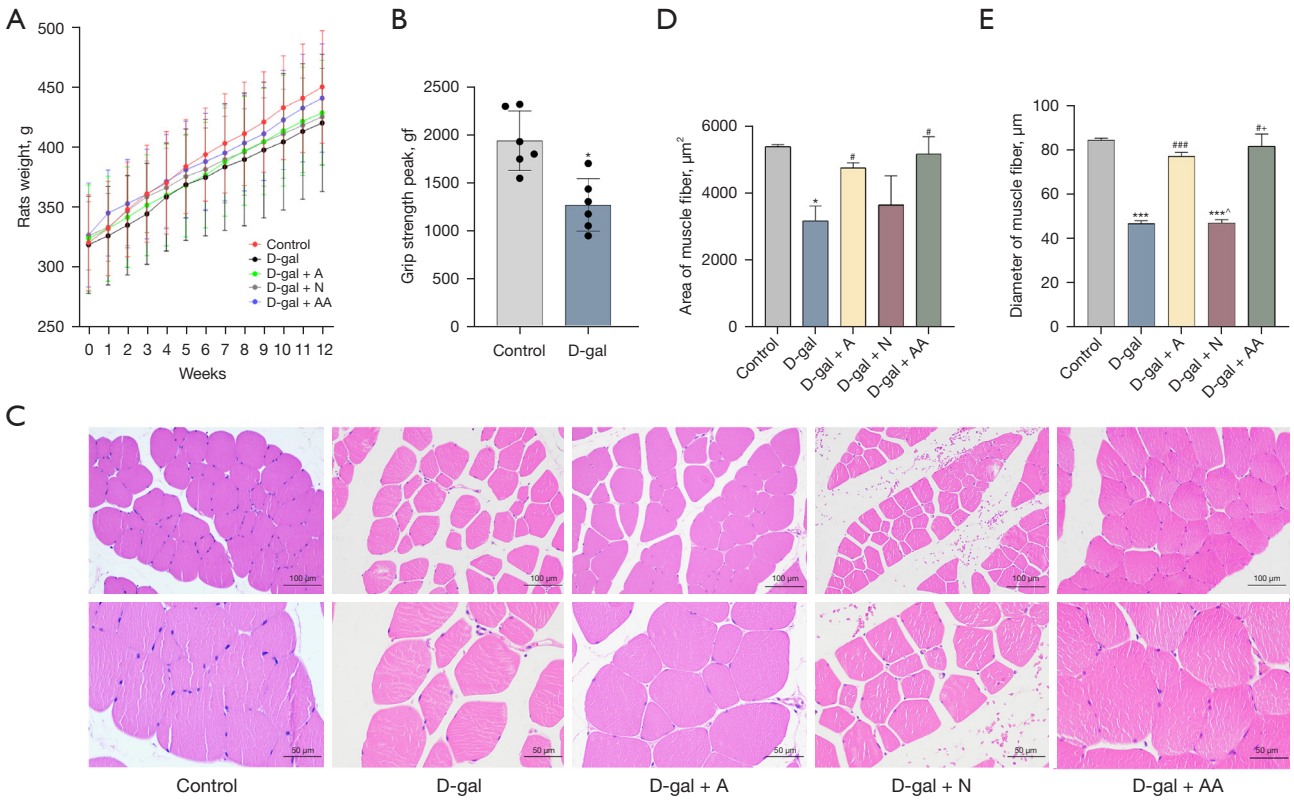

Figure 2 Evaluation of skeletal muscle atrophy in D-gal-induced aging rats through measurement of body weight (A), grip strength peak value of the four paws (B), representative myofiber cross-section of skeletal muscle stained with HE (C), cross-sectional area of skeletal muscle fibers (D), and skeletal muscle fiber diameter (E). *, P<0.05 and ***, P<0.001 relative to the control group; #, P<0.05 and ###, P<0.001 relative to the D-gal group; ^, P<0.05 relative to the DA group; +, P<0.05 relative to the DN group (n=6 for each group). gf, a unit of force; D-gal, D-galactose; A, acupuncture; N, non-acupoint; AA, amino acid; HE, hematoxylin and eosin; DA, D-gal acupuncture; DN, D-gal non-acupoint.

variance test. Data analysis was conducted using IBM SPSS Statistics 23.0 (IBM SPSS Statistics for Windows, Version 23.0. Armonk, NY, USA). A probability below 0.05 was considered statistically significant.

Results

Effect of acupuncture on atrophy in skeletal muscle

Rats receiving D-gal for 12 weeks showed a lower growth rate of B.W. and average peak grip strength than those in the control group (*Figure 2A*,*2B*). To better quantify the effects of acupuncture on skeletal muscle atrophy, skeletal muscle cross-sections were stained with H&E (*Figure 2C*) and showed rats in the D-gal group had smaller skeletal muscle area and diameter than normal rats (*Figure 2D*,*2E*, P<0.001 or P<0.05). In contrast, the cross-sectional area and skeletal muscle fiber diameter were higher after acupuncture and amino acid gavage treatments, indicating enhancement in the DA and DAA groups in comparison with the D-gal group but less improvement in the DN group (*Figure 2D*,*2E*; P<0.001 or P<0.05). In addition, the muscle fiber diameter in the DN group was shorter than the DA and DAA groups (*Figure 2D*,*2E*, P<0.05). These results indicated acupuncture could prevent D-gal from causing skeletal muscle atrophy by maintaining skeletal muscle mass and myofiber size.

Effect of acupuncture on the ultrastructure of mitochondria in skeletal muscle

Skeletal muscle ultrastructure was examined by transmission electron microscopy (TEM). While mitochondria appeared

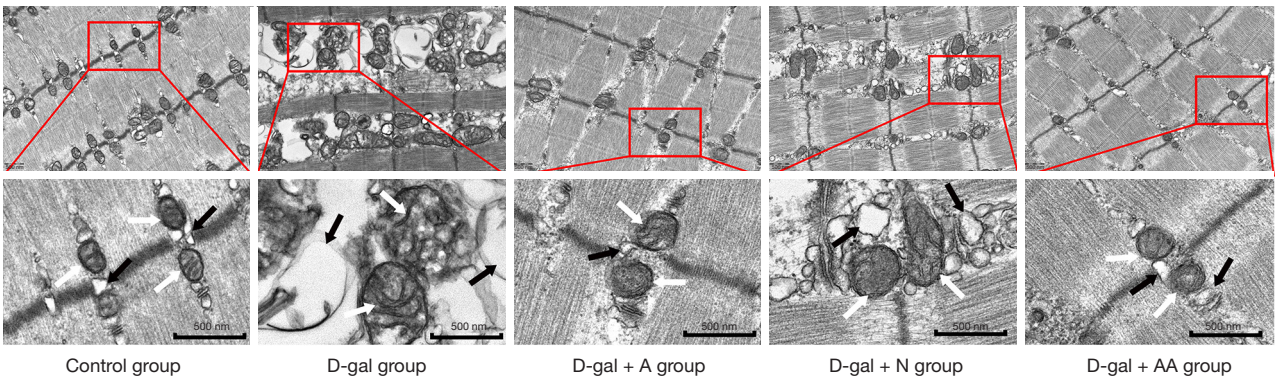

Figure 3 The microstructure of skeletal muscle was observed by TEM, ×50,000. White arrows indicate mitochondria and black arrows indicate vacuoles. Red boxed sections in the upper panels are shown enlarged in the lower panels. TEM, transmission electron microscopy; D-gal, D-galactose; A, acupuncture; N, non-acupoint; AA, amino acid.

normal in the control group, D-gal-treated rats showed many swollen mitochondria and vacuoles and abnormal and/or poorly formed mitochondria. Acupuncture and mixed amino acid administration partially reversed the mitochondrial aberrations and reduced the formation of vacuoles induced by D-gal. However, acupuncture at non-acupoints did not improve D-gal-induced mitochondrial aberration (*Figure 3*). Thus, D-gal exposure caused remarkable mitochondrial morphological distortion in skeletal muscle, and acupuncture effectively ameliorated the D-gal-induced mitochondrial morphological impairment in skeletal muscle.

Acupuncture reduced apoptosis in skeletal muscle

The apoptosis levels of skeletal muscle cells were assessed by TUNEL assay (*Figure 4A*). As shown in *Figure 4B,4C*, TUNEL staining results indicated the erector spinae in the D-gal group had substantially more apoptosis than the control group ($P<0.001$ or $P<0.05$), suggesting D-gal induction could accelerate skeletal muscle cells apoptosis. Compared to the D-gal group, the apoptotic cells number was greatly reduced by acupuncture and amino acid treatments ($P<0.001$ or $P<0.05$), while no obvious difference was observed in the apoptosis rate between the DN and the model groups. Therefore, acupuncture was efficient in reducing D-gal induced apoptosis in skeletal muscle cells.

Acupuncture reduced NF-κB p65 expression in skeletal muscle

NF-κB expression in the erector spinae sections of rats was analyzed by immunofluorescence (*Figure 5A*). Statistical analysis revealed the proportion of the positive cells and the area in skeletal muscle expressing positively for NF-κB was considerably higher than in the control group (*Figure 5B,5C*, $P<0.001$) after D-gal induction. Moreover, the positive expression rates of NF-κB in the DA and DAA groups were lower than in the D-gal group (*Figure 5B,5C*, $P<0.001$ or $P<0.01$), but there was no difference in NF-κB downregulation in the DN group (*Figure 5B,5C*, $P>0.05$). These outcomes showed acupuncture could relieve skeletal muscle atrophy by reducing the expression of NF-κB, an inflammatory factor associated with aging.

Acupuncture reduced inflammatory factors levels in skeletal muscle homogenate

According to the results of the ELISA analysis, the expression of inflammatory factors (TNF-α, IL-6, IL-1, and IL-10) was elevated by D-gal (*Figure 6A-6D*; $P<0.001$). In contrast, inflammatory factor levels in the skeletal muscle homogenate of the DA and DAA groups were lower than in the D-gal group, but the downregulation was not obvious in the DN group (*Figure 6A-6D*, $P>0.05$). Thus, acupuncture could also reduce inflammatory factor expression in the skeletal muscle homogenate.

Acupuncture inhibited miR-146a-mediated activation of related pathways

The results showed IRAK1/TRAF6/NF-κB levels were considerably elevated in the D-gal group (*Figure 7A-7F*; $P<0.001$, $P<0.01$, or $P<0.05$), while acupuncture prevented

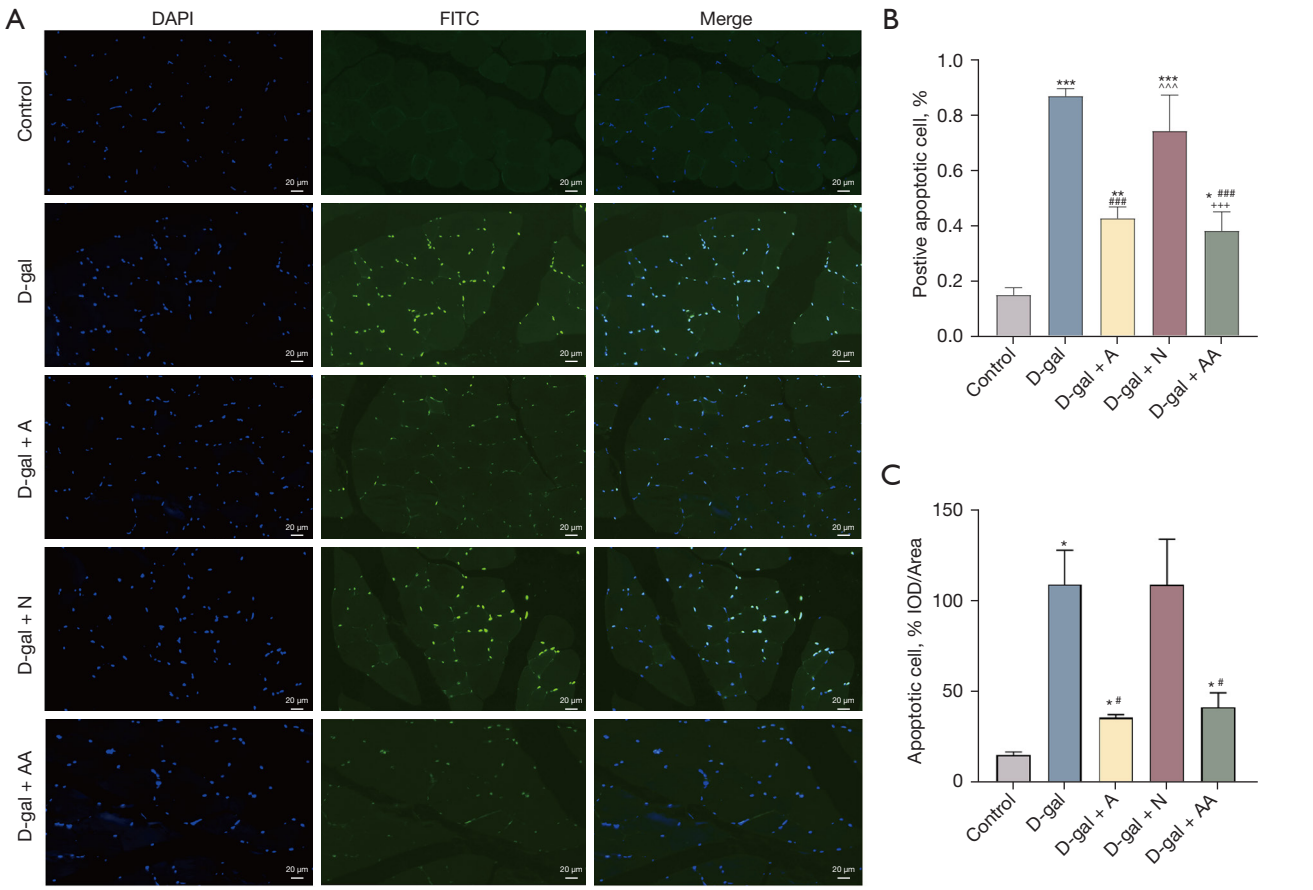

Figure 4 Effect of acupuncture treatment on apoptosis in D-gal-induced aging skeletal muscle. (A) TUNEL-stained paraspinal muscle sections of rats in each group, ×400. (B) Evaluation of the percentage of TUNEL-positive muscle cells. (C) Percentage of positive area of apoptosis in skeletal muscle after treatments. ***, P<0.001, **, P<0.01 and *, P<0.05 relative to the control group; ###, P<0.001 and #, P<0.05 relative to the D-gal group; ^^^, P<0.001 relative to the DA group; +++, P<0.001 relative to the DN group (n=5 for each group). DAPI, 4',6-diamidino-2-phenylindole; FITC, fluorescein isothiocyanate; IOD, integrated option density; D-gal, D-galactose; A, acupuncture; N, non-acupoint; AA, amino acid; TUNEL, terminal deoxynucleotidyl transferase nick-end labeling; DA, D-gal acupuncture; DN, D-gal non-acupoint.

this increase (P<0.001, P<0.01, or P<0.05). However, by comparing the D-gal group with the DN group, no statistical difference between the two groups was seen (P>0.05). The miRNA level of miR-146a was reduced in the D-gal group (*Figure 7G*; P<0.001), but acupuncture and amino acid gavage mitigated its decline (P<0.001 or P<0.05). In addition, no obvious difference in the expression level of miR146a was seen between the non-acupoint acupuncture and D-gal groups (P>0.05). Notably, acupuncture could effectively downregulate the expression of the miR-146a-mediated IRAK1/TRAF6/NF-κB pathway.

Discussion

As the global population ages, geriatric diseases become increasingly widespread. Sarcopenia is a disease of the skeletal muscle motor system with a high incidence and has been the focus of attention of researchers at home and abroad (44). This study aimed to determine if acupuncture could ameliorate aging-related skeletal muscle atrophy and alter the inflammaging process. To clarify this problem, Sprague-Dawley rats experiencing aging induced by D-gal were selected for the model group, and the morphological

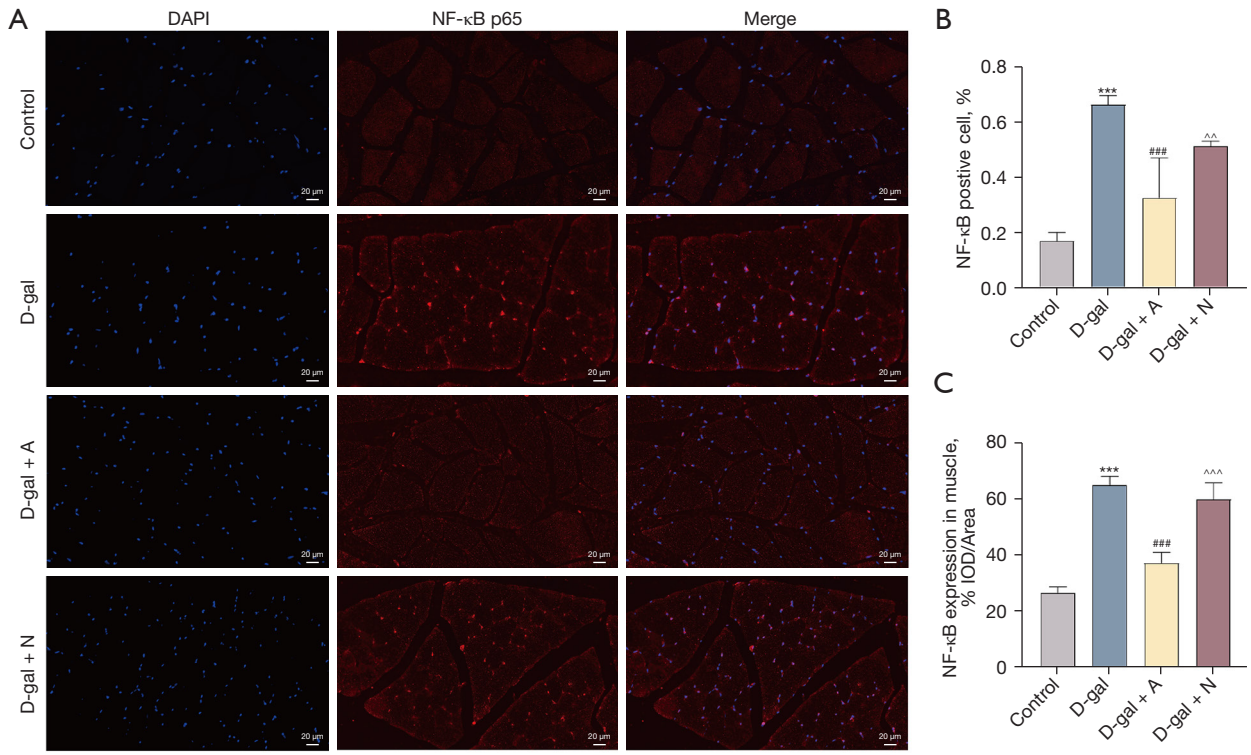

Figure 5 Effect of acupuncture treatment on NF-κB expression in D-gal-induced aging skeletal muscle. (A) The paravertebral muscle of rats in each group was harvested for fluorescent immunohistochemical staining with NF-κB (red) and DAPI (blue), ×400. (B) Evaluation of the percentage of NF-κB-positive muscle cells. (C) Percentage of the NF-κB-positive area in skeletal muscle after treatment. ***, P<0.001 relative to the control group; ###, P<0.001 relative to the D-gal group; ^^, P<0.01 and ^^^, P<0.001 relative to the DA group (n=5 for each group). DAPI, 4',6-diamidino-2-phenylindole; NF-κB, nuclear factor-kappa B; D-gal, D-galactose; A, acupuncture; N, non-acupoint; IOD, integrated option density; DA, D-gal acupuncture.W

results demonstrated the skeletal muscle fiber diameter and cross-sectional area were significantly reduced by D-gal. However, acupuncture could alleviate D-gal-induced muscle atrophy, mitochondrial aberrations, and vacuole formation in rats. The results also revealed D-gal administration increased the number of apoptotic cells in skeletal muscle, and acupuncture could alleviate cell apoptosis. In addition, we performed Western blot and qPCR detection of associated indicators to further investigate whether acupuncture had a function in the miR-146a-mediated NF-κB inflammatory pathway, and the results demonstrated it downregulated inflammatory factor expressions, including IL-10, IL-1β, TNF-α, and IL-6, and could also downregulate the miR-146a-mediated NF-κB-related inflammatory pathway.

Due to the complexity of pathophysiological alterations in sarcopenia, many existing animal models cannot completely simulate some risk factors or pathological changes in its pathogenesis. In contrast, subcutaneous injection of D-gal can affect the functional metabolism of cells by inducing oxidative stress and inflammation. This can reduce functions related to some important enzymes and induce biochemical changes similar to natural aging in experimental animals, which can be used for studying sarcopenia (45). *In vitro* investigations showed D-gal-induced skeletal muscle atrophy was accompanied by decreased muscle strength and muscle mass and induced apoptosis and autophagy impairment (46,47), and consistent with prior results, our investigation revealed subcutaneous injection of D-gal for 12 weeks accelerated skeletal muscle atrophy in rats. Furthermore, this research also showed the weight gain and grip strength of the paws in rats were reduced by D-gal.

Mitochondria are vital organelles in charge of regulating skeletal muscle metabolism. Moreover, muscle mass regulation, apoptosis susceptibility suppression, and

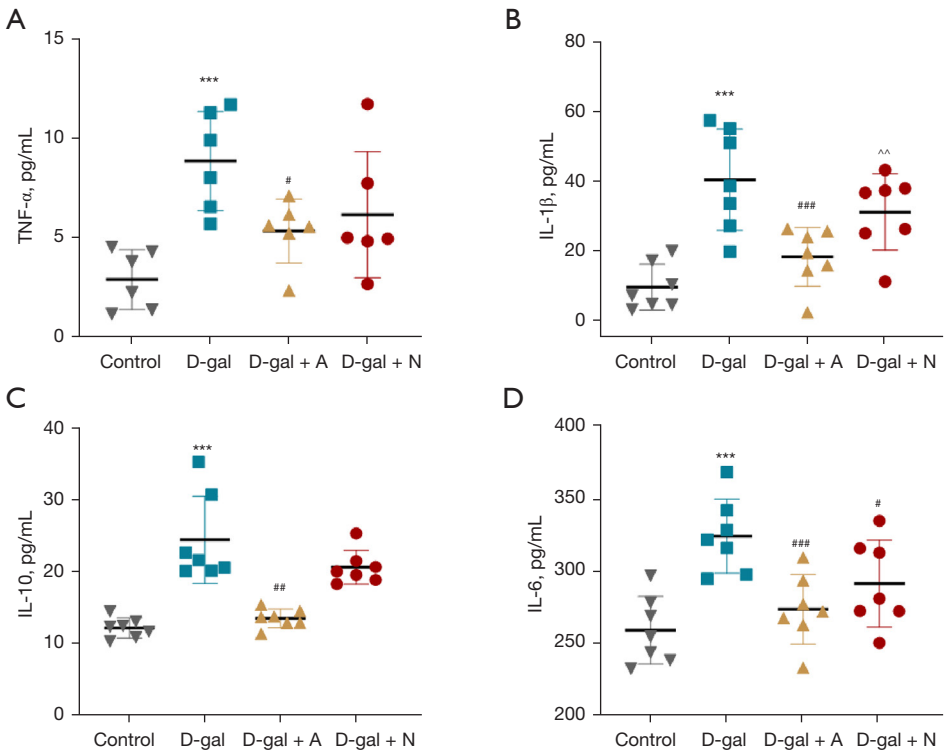

Figure 6 The expression of skeletal muscle homogenate inflammatory factors was detected by ELISA. (A-D) After 4 weeks of treatment, the expression of inflammatory factors in the skeletal muscle homogenate of rats in each group was detected by ELISA (n=6–7 each group). ***, P<0.001, relative to the normal control group; #, P<0.05, ##, P<0.01, and ###, P<0.001 relative to the D-gal group; ^^, P<0.01 relative to the DA group. TNF, tumor necrosis factor; D-gal, D-galactose; A, acupuncture; N, non-acupoint; IL, interleukin; ELISA, enzyme-linked immunosorbent assay; DA, D-gal acupuncture.

aerobic energy production management are all significantly influenced by mitochondrial turnover. Sarcopenia is partly caused by mitochondrial network dysregulation and decreased mitochondrial function (48). On one hand, the age-related impairment in signal transduction machinery sensitivity may enhance the decay rate of mitochondrial protein and mRNA, resulting in a decline in muscle mitochondrial plasticity (49). Notably, it has been shown that the buildup of damaged mitochondria causes motor neuron and muscle fiber death, emphasizing the significance of this process in the development of sarcopenia (50). On the other hand, during normal aging, muscle cells also experience the negative effects of fragmented mitochondria of low quality that generate excessive quantities of ROS, and are affected by fragmented mitochondria of low quality, creating excessive quantities of ROS (51,52), which might increase apoptosis in aged muscle (53,54). A previous study showed that under D-gal induction, muscle mitochondria were swollen and distorted, had obvious cristae disruption, and that more vacuoles appeared (47). Similar results were found in this study, which showed D-gal-induced mitochondrial malalignment and myocyte apoptosis were considerably higher in aged muscle than in normal muscular tissue. Additionally, the mitochondria of rats treated with acupuncture showed reduced mitochondrial swelling, disrupted cristae, and vacuole formation, although the disappearance of mitochondria remained unresolved. Notably, we found acupuncture could alleviate the muscle apoptosis rate of D-gal-induced aged skeletal muscle. These results imply acupuncture may postpone the skeletal muscle mitochondrial dysfunction caused by age to alleviate the apoptosis of the muscle nucleus and alleviate apoptosis.

Inflammation during aging has an impact on the onset of age-related illnesses such as sarcopenia (44). As a major mediator implicated in immunological and inflammatory responses, NF-κB content in the muscles of aged men was fourfold greater than that of young men (16), and the anterior tibialis of aged mice had an abnormal sustained

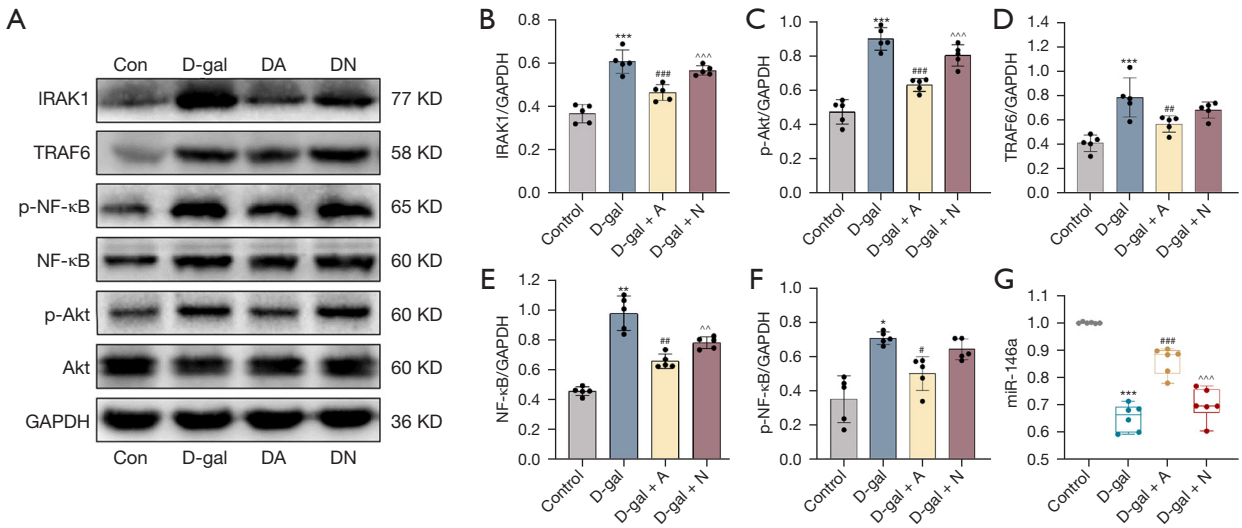

Figure 7 Acupuncture inhibited the secretion of inflammatory cytokines via the miR-146a-mediated TRAF6/NF-κB pathway. (A-F) Western blotting analysis of IRAK1/TRAF6/NF-κB/Akt protein in skeletal muscle after 4 weeks of treatment (n=5 each group). (G) The expression of miR-146a in the skeletal muscle of each rat group was detected by real-time quantitative PCR (n=6 each group). ***, P<0.001, **, P<0.01 and *, P<0.05 relative to the normal control group; ###, P<0.001, ##, P<0.01 and #, P<0.05 relative to the D-gal group; ^^^, P<0.001 and ^^, P<0.01 relative to the DA group. Con, control; D-gal, D-galactose; DA, D-gal acupuncture; DN, D-gal non-acupoint; NF-κB, nuclear factor-kappa B; PCR, polymerase chain reaction; GAPDH, glyceraldehyde-3-phosphate dehydrogenase; A, acupuncture; N, non-acupoint.

activation of NF-κB DNA binding activity during *in vivo* studies (15). A malignant inflammatory-muscular atrophy closed loop is formed with the nucleus translocation of the NF-κB p65 subunit during activation, causing the synthesis of inflammatory molecules including TNF-α and IL-6 (55,56). Accordingly, elevated levels of NF-κB, TNF-α, as well as IL-6 in the bloodstream are linked to aging and are responsible for the pathogenesis of sarcopenia (14,57,58). The effectiveness of acupuncture in anti-inflammation is highlighted by the World Health Organization (WHO), which advises the therapy for 16 different types of inflammatory illnesses (39). Notably, acupuncture has been widely shown to attenuate inflammation by downregulating TLR4 and the myeloid differentiation primary response gene 88 (MyD88) (59), promoting Sirt1 levels (60) which consequently block the receptor activator of NF-κB, and lower downstream serum inflammatory cytokines production (39) Our findings are consistent with previous results that showed the expressions of NF-κB p65 and immune mediators like TNF-α, IL-6, IL-10, and IL-1β in the skeletal muscle of rats were increased by D-gal lactose induction. Acupuncture inhibited the activation of these immune mediators and inflammatory factors. Immunofluorescence detection showed the expression of nucleus-localized NF-κB decreased significantly after acupuncture, which indicated it may reduce movement and activation of the NF-κB p65 nucleus translocation in aging skeletal muscle tissue.

Individual genetic make-up cannot solely account for the trajectory of inflammaging (61). Therefore, researchers have focused on the function of endogenous, non-coding miRNAs, which can regulate many pathophysiological processes, including cell proliferation, metabolism, and apoptosis in inflammaging (62). miR-146a shows a significant decline with aging in elderly individuals (63), and its overexpression may be generated both by replicative or stress-induced senescence and pro-inflammatory, highlighting its significant role in both inflammation and senescence (29,64). miR-146a has been shown to target molecules in the NF-κB pathway and is upregulated in response to diverse immunological mediators (65,22). It inhibits the expression of IRAK1 and TRAF6 after translation, both of which are identified as being its target genes (66). Indeed, an age-related decline in miR-146a leads to upregulated IRAK1 and TRAF6 level, which participate in the canonical NF-κB pathway, while increasing myosin

heavy chain ubiquitination and degradation, contributing to muscle atrophy, inhibition of muscle fiber regeneration, and the detrimental effects of inflammaging (11,67). Moreover, TRAF6 has been shown to activate Akt and mTOR, explaining how miR-146a influences both pathways (68). In D-gal-induced pro-aging rats, we discovered the expression of miR-146a was negatively correlated with NF-κB. In other words, after 3 months of D-gal subcutaneous injection, the miR-146a level decreased in rat muscle, while NF-κB and its associated pathway components IRAK1/TRAF6 were upregulated. Also, acupuncture upregulated miR-146a expression in D-gal-induced skeletal muscle of rats, and IRAK1/TRAF6/NF-κB signaling pathway activation and the overexpression of some inflammatory factors were reversed. This finding suggests miR-146a in skeletal muscle might be a potential target for acupuncture to control inflammation in the elderly.

Above all, our investigation gives a new viewpoint on the mechanism behind the anti-inflammatory effectiveness of acupuncture, namely improving the systemic low-grade inflammation caused by aging, and recommends acupuncture as a potential complementary therapy for sarcopenia. The specific mechanism of acupuncture to improve skeletal muscle atrophy may be achieved by may be achieved by reducing the apoptosis of muscle cells, improving the aberration of mitochondria due to aging, and exerting anti-inflammatory effects through miR-146a-mediated IRAK1/TRAF6/NF-κB signaling pathway. However, our study gives evidence of association, not causation, since we did not prove whether acupuncture ameliorates D-gal-induced muscle atrophy and inflammaging via the miR-146a-mediated IRAK1/TRAF6/NF-κB pathway. Future research should investigate the precise mechanisms behind the benefits of acupuncture treatment on aging-induced skeletal muscle atrophy via the miR-146a-mediated NF-κB pathway.

Conclusions

The results of this study reveal that 4 weeks of acupuncture inhibited D-gal-induced skeletal muscle atrophy, delayed the age-induced mitochondrial dysfunction of skeletal muscle, and alleviated apoptosis of the muscle nucleus, which may have been mediated by upregulation of an enhanced miR-146a and downregulation of the diminished expression of the IRAK1/TRAF6/NF-κB pathway. Furthermore, targeting the miR-146a-mediated IRAK1/TRAF6/NF-κB pathway by acupuncture treatment may have inhibited D-gal-induced skeletal muscle atrophy, which may provide an optimistic therapeutic strategy for less intrusive and more effective therapy for musculoskeletal disorders.

Acknowledgments

Funding: The study was funded by the National Natural Science Foundation of China (grant No. 81973924), the Youth Project of the National Natural Science Foundation of China (grant No. 81904317), and the Special Financial Subsidies of Fujian Province, China (grant No. 2021003).

Footnote

Reporting Checklist: The authors have completed the ARRIVE reporting checklist. Available at https://atm.amegroups.com/article/view/10.21037/atm-22-6082/rc

Data Sharing Statement: Available at https://atm.amegroups.com/article/view/10.21037/atm-22-6082/dss

Conflicts of Interest: All authors have completed the ICMJE uniform disclosure form (available at https://atm.amegroups.com/article/view/10.21037/atm-22-6082/coif). The authors have no conflicts of interest to declare.

Ethical Statement: The authors are accountable for all aspects of the work in ensuring that questions related to the accuracy or integrity of any part of the work are appropriately investigated and resolved. All experiments were performed under a project license (No. FJTCM IACUC 2021053) granted by Ethics Committee of Fujian University of Traditional Chinese Medicine, in compliance with institutional guidelines for the care and use of animals. A protocol was prepared before the study without registration.

References

1. Yang YF, Yang W, Liao ZY, et al. MICU3 regulates mitochondrial Ca(2+)-dependent antioxidant response in skeletal muscle aging. Cell Death Dis 2021;12:1115.
2. Larsson L, Degens H, Li M, et al. Sarcopenia: Aging-Related Loss of Muscle Mass and Function. Physiol Rev 2019;99:427-511.
3. Choi YI, Chung JW, Park DK, et al. Sarcopenia is Independently Associated with an Increased Risk of Peptic Ulcer Disease: A Nationwide Population-Based Study. Medicina (Kaunas) 2020;56:121.
4. de Blasio F, Di Gregorio A, de Blasio F, et al. Malnutrition and sarcopenia assessment in patients with chronic obstructive pulmonary disease according to international diagnostic criteria, and evaluation of raw BIA variables. Respir Med 2018;134:1-5.
5. Peball M, Mahlknecht P, Werkmann M, et al. Prevalence and Associated Factors of Sarcopenia and Frailty in Parkinson's Disease: A Cross-Sectional Study. Gerontology 2019;65:216-28.
6. Souza ABF, Nascimento DAC, Rodrigues IJM, et al. Association between sarcopenia and diabetes in community dwelling elderly in the Amazon region - Viver Mais Project. Arch Gerontol Geriatr 2019;83:121-5.
7. Xia L, Zhao R, Wan Q, et al. Sarcopenia and adverse health-related outcomes: An umbrella review of meta-analyses of observational studies. Cancer Med 2020;9:7964-78.
8. Tuttle CSL, Thang LAN, Maier AB. Markers of inflammation and their association with muscle strength and mass: A systematic review and meta-analysis. Ageing Res Rev 2020;64:101185.
9. Akbari M, Shanley DP, Bohr VA, et al. Cytosolic Self-DNA-A Potential Source of Chronic Inflammation in Aging. Cells 2021;10:3544.
10. Sendama W. The effect of ageing on the resolution of inflammation. Ageing Res Rev 2020;57:101000.
11. Li J, Yi X, Yao Z, et al. TNF Receptor-Associated Factor 6 Mediates TNFα-Induced Skeletal Muscle Atrophy in Mice During Aging. J Bone Miner Res 2020;35:1535-48.
12. Schaap LA, Pluijm SM, Deeg DJ, et al. Inflammatory markers and loss of muscle mass (sarcopenia) and strength. Am J Med 2006;119:526.e9-17.
13. Viatour P, Merville MP, Bours V, et al. Phosphorylation of NF-kappaB and IkappaB proteins: implications in cancer and inflammation. Trends Biochem Sci 2005;30:43-52.
14. Thoma A, Lightfoot AP. NF-kB and Inflammatory Cytokine Signalling: Role in Skeletal Muscle Atrophy. Adv Exp Med Biol 2018;1088:267-79.
15. Vasilaki A, McArdle F, Iwanejko LM, et al. Adaptive responses of mouse skeletal muscle to contractile activity: The effect of age. Mech Ageing Dev 2006;127:830-9.
16. Cuthbertson D, Smith K, Babraj J, et al. Anabolic signaling deficits underlie amino acid resistance of wasting, aging muscle. FASEB J 2005;19:422-4.
17. Baldwin AS Jr. Series introduction: the transcription factor NF-kappaB and human disease. J Clin Invest 2001;107:3-6.
18. Helenius M, Hänninen M, Lehtinen SK, et al. Changes associated with aging and replicative senescence in the regulation of transcription factor nuclear factor-kappa B. Biochem J 1996;318 (Pt 2):603-8.
19. Cho MJ, Kim DH, Ha S, et al. MHY2013 Modulates Age-related Inflammation and Insulin Resistance by Suppressing the Akt/FOXO1/IL-1β Axis and MAPK-mediated NF-κB Signaling in Aged Rat Liver. Appl Immunohistochem Mol Morphol 2020;28:579-92.
20. Ali A, Shah SA, Zaman N, et al. Vitamin D exerts neuroprotection via SIRT1/nrf-2/ NF-kB signaling pathways against D-galactose-induced memory impairment in adult mice. Neurochem Int 2021;142:104893.
21. Mohamadi-Zarch SM, Baluchnejadmojarad T, Nourabadi D, et al. Protective effect of diosgenin on LPS/D-Gal-induced acute liver failure in C57BL/6 mice. Microb Pathog 2020;146:104243.
22. Taganov KD, Boldin MP, Chang KJ, et al. NF-kappaB-dependent induction of microRNA miR-146, an inhibitor targeted to signaling proteins of innate immune responses. Proc Natl Acad Sci U S A 2006;103:12481-6.
23. d'Adhemar CJ, Spillane CD, Gallagher MF, et al. The MyD88+ phenotype is an adverse prognostic factor in epithelial ovarian cancer. PLoS One 2014;9:e100816.
24. Olivieri F, Lazzarini R, Babini L, et al. Anti-inflammatory effect of ubiquinol-10 on young and senescent endothelial cells via miR-146a modulation. Free Radic Biol Med 2013;63:410-20.
25. McMillan DH, Woeller CF, Thatcher TH, et al. Attenuation of inflammatory mediator production by the NF-κB member RelB is mediated by microRNA-146a in lung fibroblasts. Am J Physiol Lung Cell Mol Physiol 2013;304:L774-81.
26. Etzrodt M, Cortez-Retamozo V, Newton A, et al. Regulation of monocyte functional heterogeneity by miR-146a and Relb. Cell Rep 2012;1:317-24.

27. Boldin MP, Taganov KD, Rao DS, et al. miR-146a is a significant brake on autoimmunity, myeloproliferation, and cancer in mice. J Exp Med 2011;208:1189-201.
28. Zhao JL, Rao DS, Boldin MP, et al. NF-kappaB dysregulation in microRNA-146a-deficient mice drives the development of myeloid malignancies. Proc Natl Acad Sci U S A 2011;108:9184-9.
29. Green DR, Galluzzi L, Kroemer G. Mitochondria and the autophagy-inflammation-cell death axis in organismal aging. Science 2011;333:1109-12.
30. Krysko DV, Agostinis P, Krysko O, et al. Emerging role of damage-associated molecular patterns derived from mitochondria in inflammation. Trends Immunol 2011;32:157-64.
31. Zhou R, Yazdi AS, Menu P, et al. A role for mitochondria in NLRP3 inflammasome activation. Nature 2011;469:221-5.
32. Jang JY, Blum A, Liu J, et al. The role of mitochondria in aging. J Clin Invest 2018;128:3662-70.
33. Mason S, Wadley GD. Skeletal muscle reactive oxygen species: a target of good cop/bad cop for exercise and disease. Redox Rep 2014;19:97-106.
34. Romanello V, Sandri M. Mitochondrial Quality Control and Muscle Mass Maintenance. Front Physiol 2015;6:422.
35. Zhuang Y, Xing JJ, Li J, et al. History of acupuncture research. Int Rev Neurobiol 2013;111:1-23.
36. Thompson B, Bundell S. How electric acupuncture zaps inflammation in mice. Nature 2021. [Epub ahead of print]. doi: 10.1038/d41586-021-02806-x.
37. Feng D, Zhou H, Jin X, et al. Electroacupuncture Pretreatment Alleviates LPS-Induced Acute Respiratory Distress Syndrome via Regulating the PPAR Gamma/NF-Kappa B Signaling Pathway. Evid Based Complement Alternat Med 2020;2020:4594631.
38. Chan MWC, Wu XY, Wu JCY, et al. Safety of Acupuncture: Overview of Systematic Reviews. Sci Rep 2017;7:3369.
39. Li N, Guo Y, Gong Y, et al. The Anti-Inflammatory Actions and Mechanisms of Acupuncture from Acupoint to Target Organs via Neuro-Immune Regulation. J Inflamm Res 2021;14:7191-224.
40. Luo D, Liu L, Huang Q, et al. Crosstalk between Acupuncture and NF-κB in Inflammatory Diseases. Evid Based Complement Alternat Med 2020;2020:7924985.
41. Zhang J, Huang K, Zhong G, et al. Acupuncture Decreases NF-κB p65, miR-155, and miR-21 and Increases miR-146a Expression in Chronic Atrophic Gastritis Rats. Evid Based Complement Alternat Med 2016;2016:9404629.
42. Ruan Q, Hu X, Ao H, et al. The neurovascular protective effects of huperzine A on D-galactose-induced inflammatory damage in the rat hippocampus. Gerontology 2014;60:424-39.
43. Yu SG, Guo Y. Experimental Acupuncture Science. Shanghai: Shanghai Scientific & Technical Publishers, 2009.
44. Cruz-Jentoft AJ, Sayer AA. Sarcopenia. Lancet 2019;393:2636-46.
45. Xie WQ, He M, Yu DJ, et al. Mouse models of sarcopenia: classification and evaluation. J Cachexia Sarcopenia Muscle 2021;12:538-54.
46. Kou X, Li J, Liu X, et al. Ampelopsin attenuates the atrophy of skeletal muscle from d-gal-induced aging rats through activating AMPK/SIRT1/PGC-1α signaling cascade. Biomed Pharmacother 2017;90:311-20.
47. Chang L, Liu X, Liu J, et al. D-galactose induces a mitochondrial complex I deficiency in mouse skeletal muscle: potential benefits of nutrient combination in ameliorating muscle impairment. J Med Food 2014;17:357-64.
48. Hood DA, Memme JM, Oliveira AN, et al. Maintenance of Skeletal Muscle Mitochondria in Health, Exercise, and Aging. Annu Rev Physiol 2019;81:19-41.
49. Carter HN, Kim Y, Erlich AT, et al. Autophagy and mitophagy flux in young and aged skeletal muscle following chronic contractile activity. J Physiol 2018;596:3567-84.
50. Sonjak V, Jacob KJ, Spendiff S, et al. Reduced Mitochondrial Content, Elevated Reactive Oxygen Species, and Modulation by Denervation in Skeletal Muscle of Prefrail or Frail Elderly Women. J Gerontol A Biol Sci Med Sci 2019;74:1887-95.
51. García-Prat L, Martínez-Vicente M, Perdiguero E, et al. Autophagy maintains stemness by preventing senescence. Nature 2016;529:37-42.
52. Wu JJ, Quijano C, Chen E, et al. Mitochondrial dysfunction and oxidative stress mediate the physiological impairment induced by the disruption of autophagy. Aging (Albany NY) 2009;1:425-37.
53. Dirks AJ, Hofer T, Marzetti E, et al. Mitochondrial DNA mutations, energy metabolism and apoptosis in aging muscle. Ageing Res Rev 2006;5:179-95.
54. Lin MT, Beal MF. Mitochondrial dysfunction and oxidative stress in neurodegenerative diseases. Nature 2006;443:787-95.
55. Baker RG, Hayden MS, Ghosh S. NF-κB, inflammation, and metabolic disease. Cell Metab 2011;13:11-22.
56. Lawrence T. The nuclear factor NF-kappaB pathway in inflammation. Cold Spring Harb Perspect Biol

2009;1:a001651.
57. Dalle S, Rossmeislova L, Koppo K. The Role of Inflammation in Age-Related Sarcopenia. Front Physiol 2017;8:1045.
58. Beyer I, Mets T, Bautmans I. Chronic low-grade inflammation and age-related sarcopenia. Curr Opin Clin Nutr Metab Care 2012;15:12-22.
59. Wang L, Yang JW, Lin LT, et al. Acupuncture Attenuates Inflammation in Microglia of Vascular Dementia Rats by Inhibiting miR-93-Mediated TLR4/MyD88/NF-κB Signaling Pathway. Oxid Med Cell Longev 2020;2020:8253904.
60. Ma B, Li P, An H, et al. Electroacupuncture Attenuates Liver Inflammation in Nonalcoholic Fatty Liver Disease Rats. Inflammation 2020;43:2372-8.
61. Olivieri F, Prattichizzo F, Giuliani A, et al. miR-21 and miR-146a: The microRNAs of inflammaging and age-related diseases. Ageing Res Rev 2021;70:101374.
62. Slota JA, Booth SA. MicroRNAs in Neuroinflammation: Implications in Disease Pathogenesis, Biomarker Discovery and Therapeutic Applications. Noncoding RNA 2019;5:35.
63. Bhaumik D, Scott GK, Schokrpur S, et al. MicroRNAs miR-146a/b negatively modulate the senescence-associated inflammatory mediators IL-6 and IL-8. Aging (Albany NY) 2009;1:402-11.
64. Sugimoto MA, Sousa LP, Pinho V, et al. Resolution of Inflammation: What Controls Its Onset? Front Immunol 2016;7:160.
65. Poli G, Fabi C, Bellet MM, et al. Epigenetic Mechanisms of Inflammasome Regulation. Int J Mol Sci 2020;21:5758.
66. Bertolet G, Kongchan N, Miller R, et al. MiR-146a wild-type 3' sequence identity is dispensable for proper innate immune function in vivo. Life Sci Alliance 2019;2:e201800249.
67. Mensà E, Giuliani A, Matacchione G, et al. Circulating miR-146a in healthy aging and type 2 diabetes: Age- and gender-specific trajectories. Mech Ageing Dev 2019;180:1-10.
68. Yang WL, Wang J, Chan CH, et al. The E3 ligase TRAF6 regulates Akt ubiquitination and activation. Science 2009;325:1134-8.

(English Language Editor: B. Draper)

Cite this article as: Jin J, Yang Z, Liu H, Guo M, Chen B, Zhu H, Wang Y, Lin J, Wang S, Chen S. Effects of acupuncture on the miR-146a-mediated IRAK1/TRAF6/NF-κB signaling pathway in rats with sarcopenia induced by D-galactose. Ann Transl Med 2023;11(2):47. doi: 10.21037/atm-22-6082